Int. J. Electrochem. Sci., 9 **(2014)** 4776 - 4792

International Journal of
ELECTROCHEMICAL
SCIENCE
www.electrochemsci.org

Actuation Behaviour of a Derivatized Pyrrole Accordion Type Polymer

Meryck Ward, Shanielle Botha, Emmanuel Iwuoha, Priscilla Baker[*]

SensorLab, Chemistry Department, Faculty of Science, University of the Western Cape, Private Bag X17, Bellville 7535, South Africa
[*]E-mail: pbaker@uwc.ac.za

Received: 26 March 2014 / *Accepted:* 15 May 2014 / *Published:* 16 June 2014

A monomer (Phenazine-2,3-diimino(pyrrole-2-yl)–PDP) derived from the condensation reaction between 2,3-diaminophenazine and a pyrrole derivative has been synthesized as a hinge molecule in the design of a zig-zag polymer. The monomer was polymerized both chemically and electrochemically in order to produce the polymer material, phenazine-2,3-diimino(pyrrole-2-yl (PPDP). During electrochemical polymerization the system was doped using 1,4-napthaquinone sulphonic acid (NQSA) and polyvinylsulfonic acid (PVSA) respectively, to improve conductivity. Characterization of the materials by Fourier transform infrared spectroscopy (FTIR) confirmed the successful linking of the starting materials to produce the hinge molecule and nuclear magnetic resonance spectroscopy (NMR) supported the FTIR data. The electrochemistry of the polymer in the doped and undoped state was evaluated using cyclic voltammetry (CV) and electrochemical impedance spectroscopy (EIS).

Keywords: zig-zag polymer, 1,4-napthaquinone sulphonic acid, polyvinylsulfonic acid, fourier transform infrared, nuclear magnetic resonance, cyclic voltammetry, electrochemical impedance spectroscopy, electron transfer, diffusion coefficient.

1. INTRODUCTION

Polypyrrole (PPy) and its derivatives are the most extensively studied conducting polymers due to the easily oxidizable monomer that is soluble in water, commercially available, the high electrical conductivity, good electrochemical properties, thermal stability and the high mechanical strength which is easily generated both chemically and electrochemically [1]. Intrinsic properties of polypyrrole include environmental stability, good redox and conductivity behavior [2] have been utilized in many

applications, including batteries, supercapacitors, electrochemical (bio) sensors, conductive textiles and fabrics, drug delivery systems and mechanical actuators [3-5].

Oxidation of a p-doped polymer can maintain electroneutrality via two methods. The polymer can be doped with mobile cations and anions. The insertion and removal of anions during the redox reaction will maintain the neutrality along the polymer backbone [6]. Otero et al. developed a model that explains the volume changes in conducting polymers taking into account the electrostatic repulsion between charged polymeric chains [7]. According to this model, when a conducting polymer is oxidized, positive charges are generated along the polymeric chains. These positive charges produce electrostatic repulsions between the chains, resulting in conformational changes in the polymeric structure. These free spaces are formed due to conformational changes which facilitate the insertion of solvated counter-anions, maintaining the electroneutrality of the polymer resulting in an increase in its volume. Thus upon oxidation of a conducting polymer doped with a small mobile anion, its volume increases proportionally to the formed positive charges (expansion). When the conducting polymer is reduced the positive charges are neutralized by the addition of electrons from the potentiostat. The electrostatic repulsions are eliminated, diminishing the free space and counter ions expelled from the chain to maintain the electroneutrality in the polymer. Thus, upon reduction, its volume decreases (contraction).

Conducting polymers are suitable for the production of actuator systems with various designs (bilayer, trilayer and interpenetrating polymer networks) because of low operation voltages (~1V), large stress (higher than that of natural muscles), large strain, the possibility to fabricate actuators in different shapes (fibres, yarns, films, tubes, multilayers), good work density per cycle, high degree of compliance and good lifetime [8-10]. Actuator designs incorporating electroactive polymers display the best desired properties with respect to actuation displacement, fracture toughness, density and reaction speed. Electroactive polymer materials displayed favourable properties with respect to displacement capacity which are comparative to human muscle movements [11].

Different polypyrrole actuator devices have been synthesized over the past two decades, showing properties matching and even exceeding that of natural muscles. Polypyrrole is electrochemically driven and can be constructed in linear or bending (bilayer) actuators. In linear actuators, the actuation mechanism is based on the longitudinal expansion and contraction of the polymer due to the insertion and de-insertion of ions. A PPy film doped with benzenesulfonate anions (BS^-) was characterized electrochemically by Della Santa [12]. This polymer film was obtained under the trade name Lutamer and underwent swelling that produced a linear dimension change by 2%. Other linear polypyrrole actuators include PPy-DBS, PPy-tetrafluoroborate [13] and PPy-hexafluorophosphate [14].

In this work we present the synthesis and characterization of a hinged polypyrrole actuator. The linking molecule (hinge) is phenazine with interconnected dipyrrole units. Voltammetry was used to assess the effect of the dopant (NQSA and PVSA) on electron mobility in the electro-polymerized thin film polymers in aqueous solution. Electrochemical impedance spectroscopy was used to assess the capacitance changes during oxidation and reduction as a quantitative measure of actuation.

2. EXPERIMENTAL

2.1. Synthesis of phenazine-2,3-diimino (pyrrole-2-yl) monomer

Phenazine-2,3-diimino(pyrrole-2-yl) was chemically synthesized by the condensation reaction of 2.1 mmol pyrrole-2-carboxaldehyde and 1 mmol of 2,3-diamino phenazine in acetic acid for 48 hours under reflux (scheme 1) with a yield of 61 %. The temperature used for the setup was 130 °C as the boiling point of the acetic acid is 120 °C.

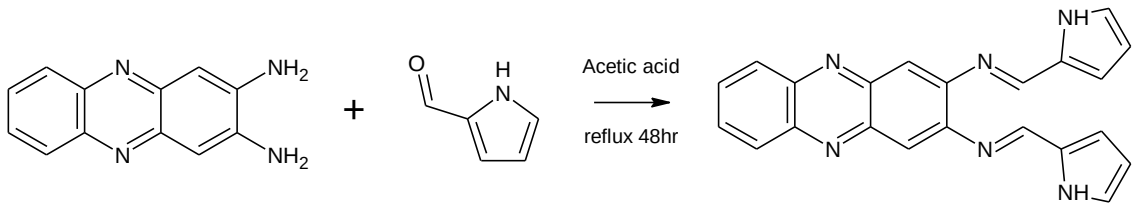

Scheme 1. Starting materials undergoing a reflux condensation reaction to produce the new monomer material.

2.2. Polymerization to form poly(phenazine-2,3- diimino (pyrrole-2-yl))

The material was synthesized by chemical and electrochemical polymerization. Chemically the polymer was prepared by reacting 0.5 mmol PDP (monomer) and 5 mmol Anhydrous Iron (III) Chloride ($FeCl_3$). The $FeCl_3$ solution was added dropwise to the already stirring PDP solution (reaction between $FeCl_3$ and water was exothermic). The solution was allowed to stir for 24 hours before filtration and washing with methanol.

The polymerization solution was prepared by dissolving the monomer material in 2 mL of Dimethylformamide (DMF) and then dilued to 4 mL with 0.1 M Hydrochloric Acid (HCl). Growth was allowed to occur with an increase in scan cycles, 25 polymerization cycles were used. NQSA and PVSA were used as the dopants during polymerization. Polymerization material containing the NQSA was prepared on a glassy carbon eletrode (GCE) whereas the PVSA material was prepared on a screen print carbon electrode (SPCE). The reference electrode was Ag/AgCl and a platinum counter electrode was used.

2.3. Characterization of monomer and electrochemically synthesised polymer material.

FTIR characterization was performed on starting materials **(**pyrrole-2-carboxaldehyde and 2,3-diaminophenazine) and monomer by placing the solid material in the path of IR beam. NMR analysis was performed by dissolving the materials in DMSO-d^6, ^{1}H NMR was used for sample analysis. Electrochemically synthesized polymer material was characterized by cyclic voltammetry in 0.1 M HCl solution at different scan rates. The material was then quantitatively assessed by calculating; peak separation, electron transfer, formal potentials, current ratios and diffusion coefficients.

Electrochemical impedance spectroscopy of the PPDP-NQSA and PPDP-PVSA were performed between -500 mV to 500 mV using 100 mV steps,

3. RESULTS AND DISCUSSION

3.1. FTIR Analysis

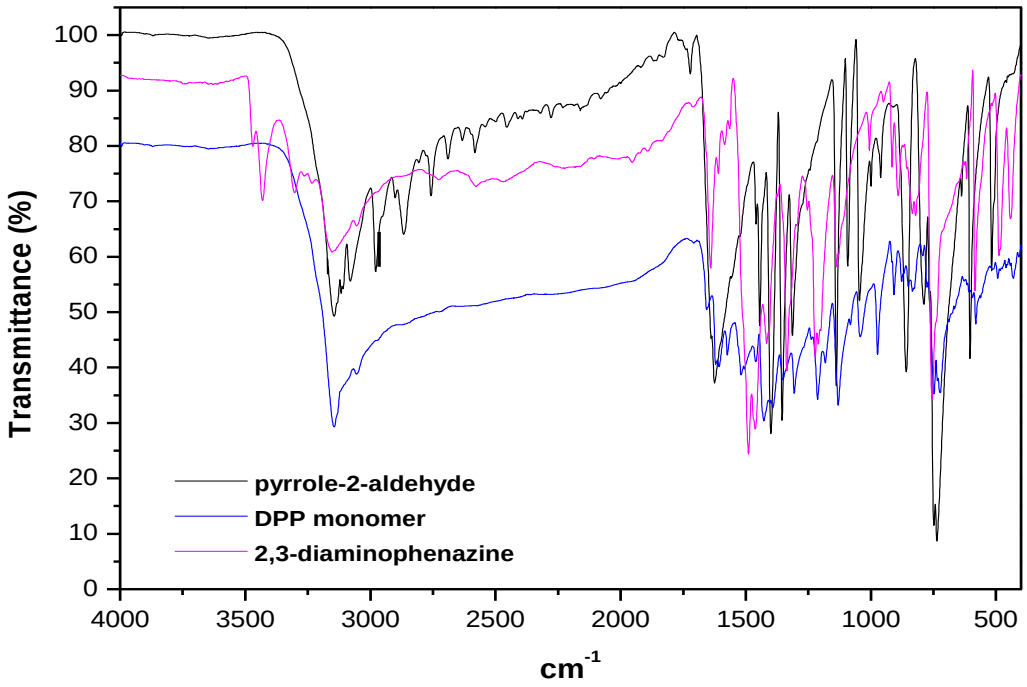

Figure 1. FTIR spectra of pyrrole-2-carboxaldehyde; DAP and PDP

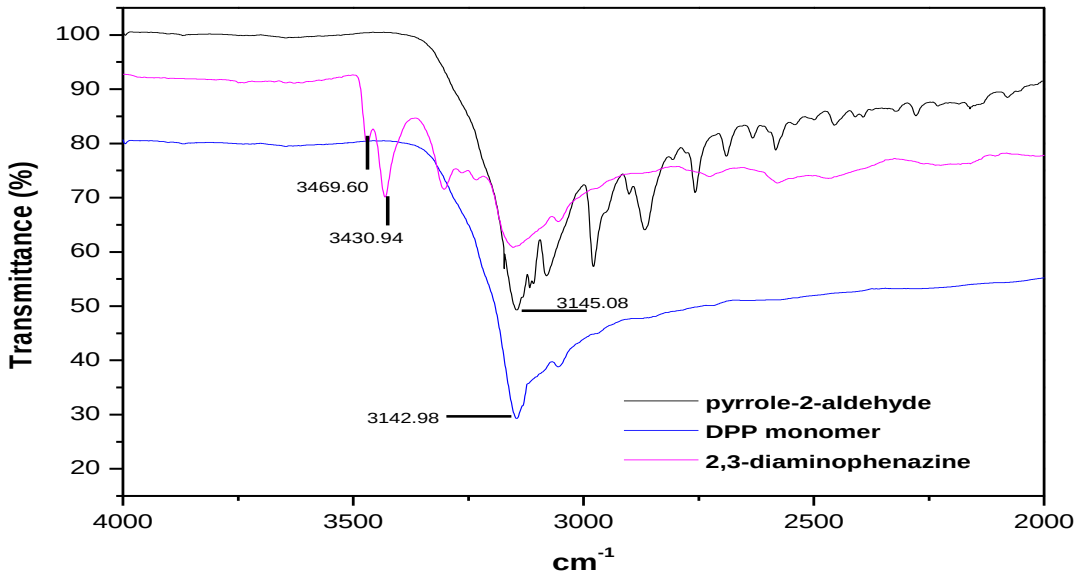

Figure 2. FTIR spectra of pyrrole-2-carboxaldehyde; DAP and PDP between 4000 and 2000cm^{-1}.

The FTIR spectra of DAP, showed 2 peaks at 3469.6 cm^{-1} and 3430.94 cm^{-1} respectively, indicative of a NH_2 stretching vibration (figure 2). This peak is not seen in the FTIR spectra of PDP and thus the NH_2 bond is not present in the chemical structure of PDP. The FTIR spectra of pyrrole-2-carboxaldehyde, shows a peak at 3145 cm^{-1}, which is characteristic of a NH stretching vibration. This peak is still present in the FTIR spectra of PDP (3142 cm^{-1}), indicating the NH bond of PDP. A peak at 738 and 727 cm^{-1} is observed for both pyrrole-2-carboxaldehyde and PDP, which is indicative of an unsubstituted α- position in pyrrole.

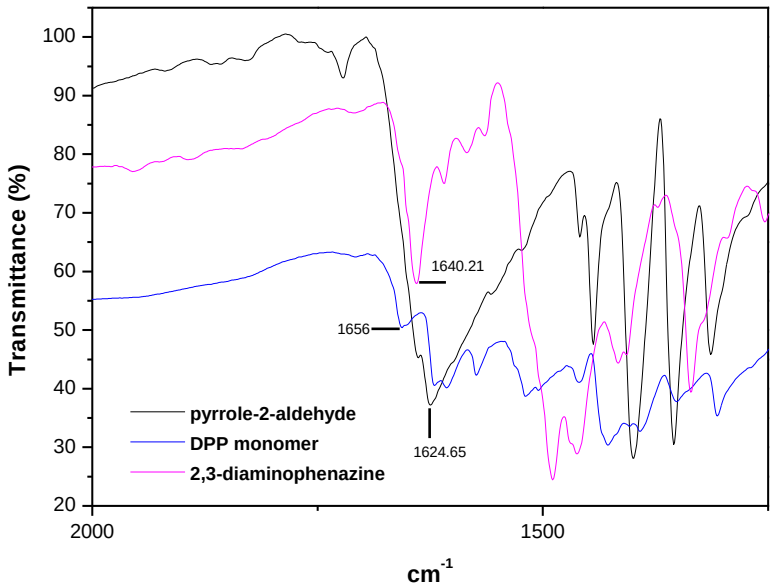

Figure 3. FTIR spectra of pyrrole-2-carboxaldehyde; DAP and PDP between 2000 and 1250cm^{-1}.

The spectra of pyrrole-2-carboxaldehyde displays a prominent peak at 1624.65 cm^{-1}, which is associated with the C=O stretching band (figure 3).

Table 1. FTIR spectra peak assignment

pyrrole-2-carboxaldehyde	
Assignment	Frequency (cm^{-1})
NH- stretch	3145
C=O stretch	1624
Unsubstituted α – position	738
2,3- diaminophenazine	
C=N stretch	1640
NH_2 stretch	3469 and 3430
Phenazine-2,3- diimino (pyrrol-2-yl)	
C=N stretch	1656
NH- stretch	3142
Unsubstituted α – position	727

The spectra of PDP does not show this peak, indicating that the C=O bond is absent in the structure of PDP. Peaks observed at 1640.21 cm^{-1} and 1656 cm^{-1} were associated with DAP and PDP respectively. This is as a result of a C=N stretching band present in both compounds (table 1). All the results from FTIR substantiate the formation of the desired product, with the chemical structure as shown in reaction 1.

3.2. NMR Analysis

Table 2. NMR data assignment, ^{1}H NMR (DMSO-d^6):

δ-shift	Assignment
pyrrole-2-carboxaldehyde	
5.328	1H, m, 3-H
6.063	1H, d, 4-H
6.270	1H, m, 2-H
8.528	1H, s, 5-H
11.152	1H, d, 1-H
2,3- diaminophenazine (DAP)	
1.528	4H, s, 1-H and 1'-H
5.281	2H, s, 2-H and 2'-H
5.925	2H, m, 4-H and 4'-H
6.586	2H, d, 3-H, 3'-H
Phenazine-2,3-diimino(pyrrol-2-yl) (PDP)	
5.228	4H, m, 3-H, 3'-H, 4-H and 4'-H
5.670	2H, m, 2-H and 2'-H
5.925	2H, m, 5-H and 5'-H
6.180	2H, m, 8-H and 8'-H
6.428	2H, d, 7-H and 7'-H
6.588	2H, s, 6-H and 6'-H
11.153	2H, m, 1-H and 1'-H

The ^{1}H NMR spectrum of pyrrole-2-carboxaldehyde showed the aldehydic proton as a singlet at δ 8.528 (table 2). This singlet disappears in the spectrum of PDP and is seen at in the high field region at δ 5.925, indicating that the C=O bond of DAP is not present, as expected for the desired product. The ^{1}H NMR spectrum of DAP showed the 1-NH_2 and 1'- NH_2 singlet at δ 1.528. This peak disappears in the spectrum of PDP, substantiating the formation of PDP. Figure 4 represents the proposed accordion structure, based on the bond formation confirmed by spectroscopic data.

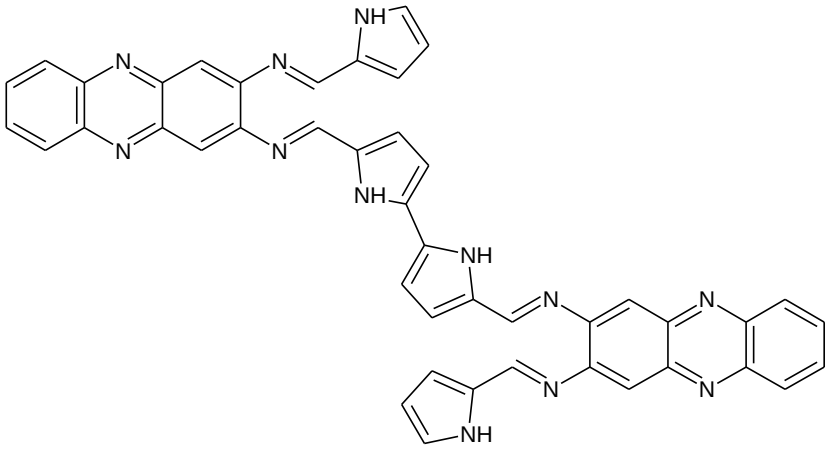

Figure 4. Structure of the zig-zag polymer material.

3.3. Cyclic Voltammetry

Undoped polypyrrole, electrochemically synthesized from aqueous acidic solutions showed rather poor redox performance, characterized by indistinct redox peaks as measured by cyclic voltammetry. However the addition of surfactant ions such as 1,4-napthaquinone sulphonic acid greatly improves the electrochemistry of the polymer and the formal potential for the doped polypyrrole was determined to be 322 mV vs Ag/AgCl (figure 5) [15].

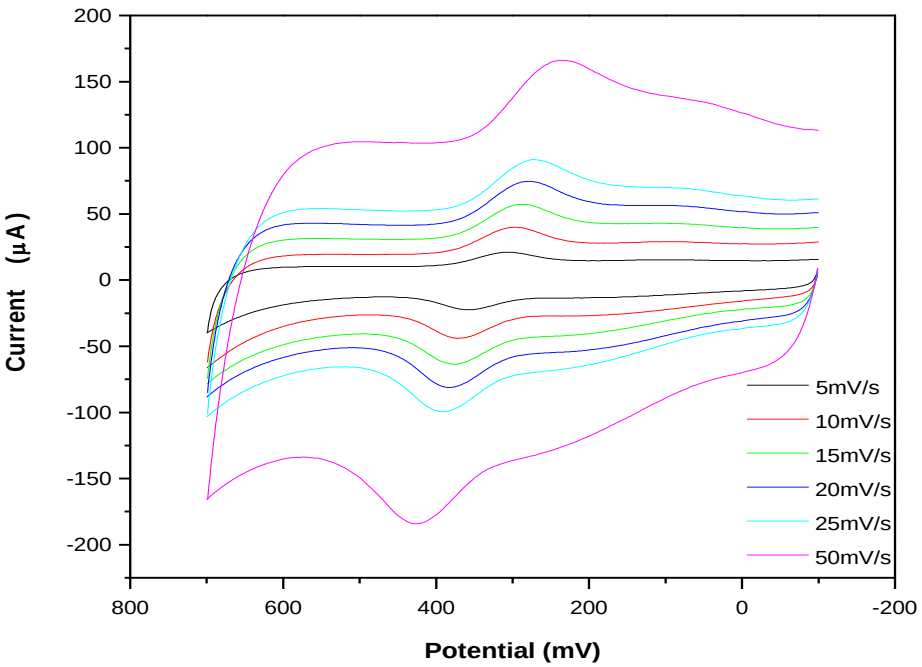

Figure 5. Multi-scan rate voltammogram obtained at a glassy carbon electrode with a thin film of PPy-NQSA in 0.1 M HCl at scan rates of 5-50 mV/s.

Over oxidation and degradation of polypyrrole occurred at high potentials, whilst extremely negative potentials led to the evolution of hydrogen [16]. Thus the potential window of -600 mV to +700mV was developed as an optimum range. The electrochemically polymerized PPDP-NQSA grown at 50mV/s for 25 cycles showed good adherence to the glassy carbon electrode surface, as is indicated by an increase in peak current with very small change in potential, for all peaks observed (figure 6). The increase in polymerization current as the number of CV cycles increased was indicative of conductive thin film formation.

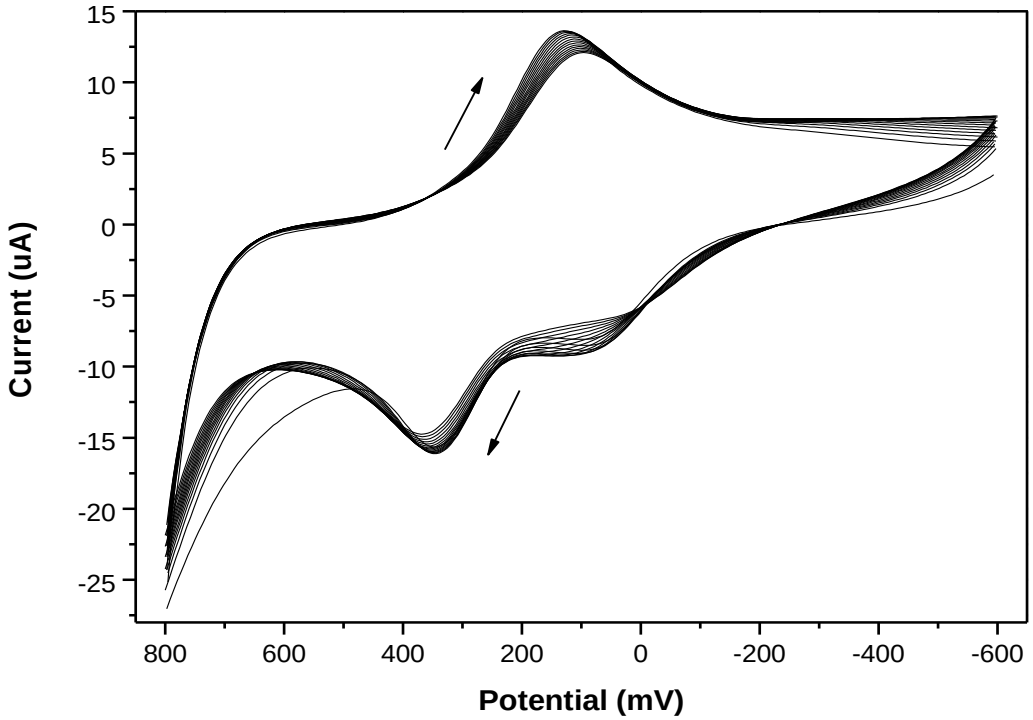

Figure 6. Polymerization of GC/PPDP-NQSA from 1 mM PDP in 0.1 M HCl/DMF (1:1).

The cyclic voltammogram of the doped PPDP polymer showed two distinctive redox couples (figure 7). The anodic peak and cathodic peak potential of PPy-NQSA were observed at +364 mV and +301 mV respectively [17]. From the multi-scan rate voltammogram of PPDP-NQSA at 50 mV/s, it was observed that the anodic peak potential *a,* is at +386 mV and the cathodic peak potential *a*' was at +298 mV. These potentials were fund to be similar to that of PPy-NQSA and thus the redox couple *a: a'* was attributed to the electrochemistry of pyrrole. The second irreversible redox couple displayed only one peak, i.e. the anodic potential at +99 mV at a scan rate of 50 mV/s. Thus, peak *b* and its irreversible couple *b*' was attributed to the electrochemistry of the phenazine moiety. DAP polymerized in various solvents displayed irreversible redox activity between -800 mV to -200 mV [18-19].

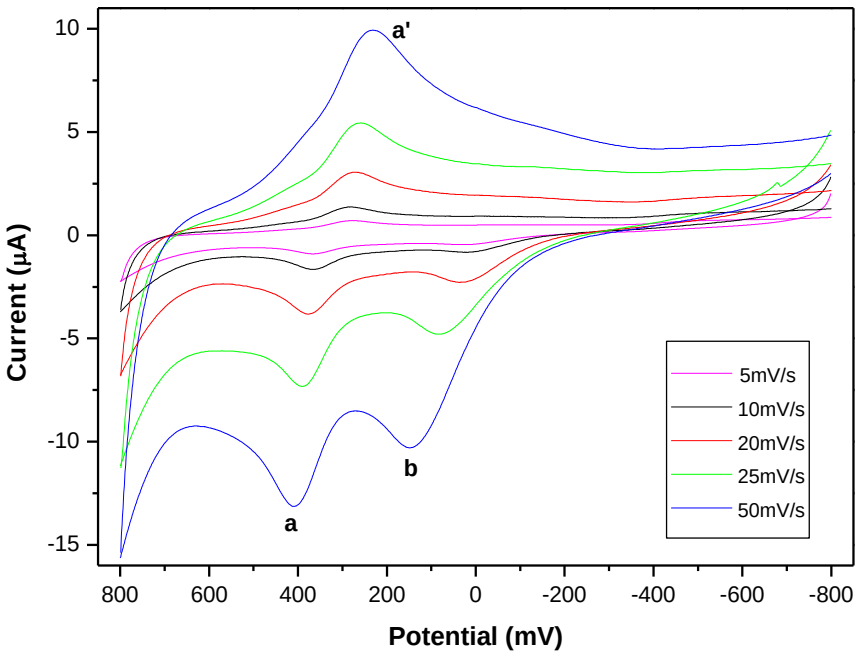

Figure 7. Multi- scan rate voltammogram obtained at a glassy carbon electrode with a thin film of PPDP-NQSA in 0.1M HCl at scan rates of 5- 50 mV/s.

The ratio of Ipc/Ipa ranged from 0.78 for 5 mV/s to 0.76 at 100 mV/s for *a*:*a*', suggesting a one electron system. The peak separation for the redox couple *a:a'* at 5 mV/s is +63 mV vs Ag/AgCl, is indicative of a quasi- reversible process. This also indicated that the polymer was bound to the surface since $\Delta E_p = (E_{pa} - E_{pc})$ should be less than 63 mV for a surface bound species [20-21]. The seperation increased progressively from 60 mV at 5 mV/s to 12 6mV at 100 mV/s coupled with an increase in the magnitude of the peak currents with an increase scan rates. This showed that the peak currents were diffusion controlled and that diffusion of electrons took place across the polymer chain, via the conjugated system of pyrrole and phenazine.

The Brown-Anson equation (equation 1) was used to estimate the surface concentration of the polymer ($\Gamma^*_{PPDP\text{-}NQSA}$) by plotting the peak currents (I_p) obtained at different scan rates (v), between 5 mV/s and 50 mV/s, vs. the scan rates [22].

$$ip = n^2 F^2 \Gamma^*_{PPDP\text{-}NQSA} (A\, v/4RT) \ldots\ldots \text{(equation 1)}$$

The notations F, A, R and T denotes the Faraday constant (96584 $C.mol^{-1}$), working electrode area (0.071 cm^2), molar gas constant (8.314 $J.K^{-1}.mol^{-1}$ and room temperature (298 K) respectively. Brown Anson plots confirmed the formation of a stable film whose density or surface concentration, was slightly lower during reduction (1.5×10^{-9} $mol.cm^{-2}$) as compared to oxidation (1.89×10^{-9} $mol.cm^{-2}$) (redox couple *a:a'*). The plots showed a linear regression coefficient (r^2) of 0.999, 0.997 and 0.990 respectively for anodic peak *a*', cathodic peak *a* and anodic peak *b* vs. scan rates.

The Randle-Sevcik equation was applied to this diffusion controlled system, to determine the diffusion coefficient (D_e), by plotting peak current vs. square root of the scan rate [23].

D_e, which is a measure of electron transfer along the polymer chain, was found to be 4.62 x $10^{-7}cm^2.s^{-1}$, 4.61 x $10^{-7}cm^2.s^{-1}$ and 4.39 x $10^{-7}cm^2.s^{-1}$ for the anodic peak *a*', cathodic peak *a* and anodic peak *b* respectively. The values of D_e for both *a* and *a'* are similar, indicating that the deviation from full reversibility does not involve permanent electronic changes in the bulk polypyrrole film upon cycling. Thus some other process occurred in the film which is responsible for the kinetics observed [17].

The cyclic voltammogram at a scan rate of 5mV/s was used to determine the rate constant (k_0) for electron transfer within the polymer chain using the Nicholson treatment for a quasi-reversible electrochemical system using equation 6 [23-24]. The transfer coefficient, α, of 0.5 was assumed for the PPDP-NQSA system and the kinetic parameter, ψ (dimensionless), was assigned a value of 7 based on the peak seperation (ΔE_p) of 60 mV at a scan rate of 5mV/s. The k_0 value of 1.48 x 10^{-3} $cm.s^{-1}$ was obtained for the polymer at 5mV/s at all the peak potentials, which confirmed the electroactivity of the species. This also indicated that electron hopping along the polymer chain at low scan rate was quite facile. These values are comparable to rate constants of other sulfonated doped polypyrrole conducting polymers, i.e. 2.20 x 10^{-3} cm. s^{-1} for PPy-NQSA and 3.75 x 10^{-2} cm. s^{-1} for PPy-NSA [25]. Other conducting polymers with similar rate constants have been reported i.e. polyaniline with a k_o value of 5.4 x 10^{-3} $cm.s^{-1}$[26] and poly(ethylenedioxythiophene) with a k_o value of 1.5 to 45.3 x 10^{-3} $cm.s^{-1}$ [27].

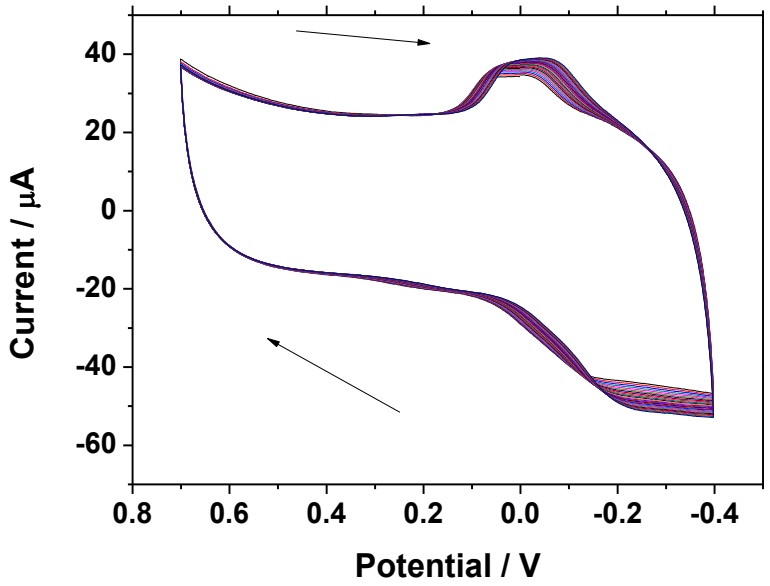

Figure 8. Polymerization voltammagram of screen print carbon electrode onto which the PPDP-PVSA was polymerized by using a solution containing 1 mM PDP in 0.1 M HCl/ DMF (1:1), with PVSA acting as the surfactant.

Polymerization of the monomer material was performed to produce the polymer material poly(phenazine-2,3-diimino(pyrrole-2-yl)), which was electropolymerized (figure 8) onto the surface of a screen printed carbon electrode (SPCE). The current of the developing polymer film increased with the number of cycles and the polymer was produced after 25 cycles. The respective characterization of this material was performed in a 0.1 M HCl solution (figure 9), with one redox

couple A-A' due to one electron transfer at -50 mV and -45 mV and a redox couple B-B' which resulted from the absorbance of undissolved material onto the surface of the electrode.

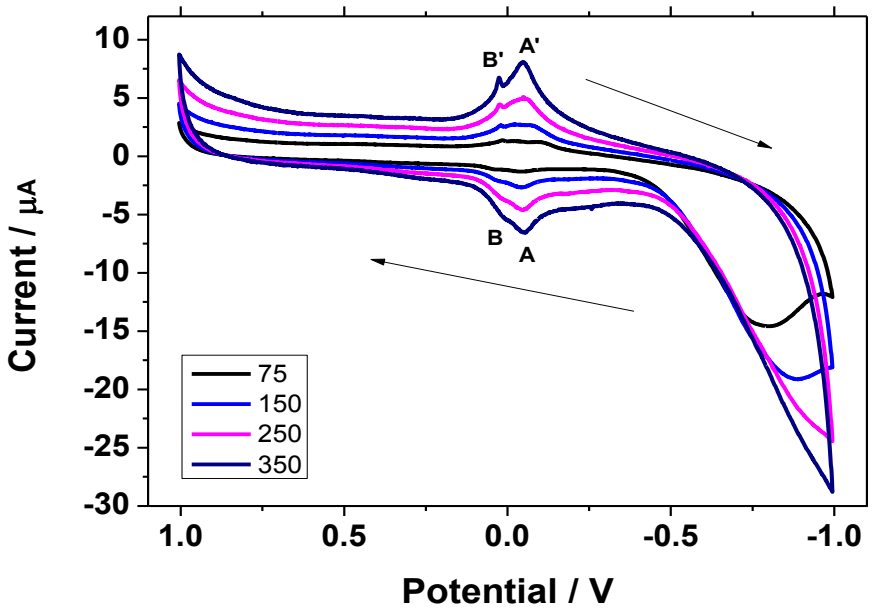

Figure 9. PPDP-PVSA characterization in 0.1 M HCl, scan rates; 75 - 350 mV/s

Table 3. Peak current response for PPDP-PVSA in HCl, from cyclic voltammetry.

Scan Rate	ipa / µA (A)	ipc / µA (A')	ipa/ipc (A-A')
75	1.3511	1.1609	1.16
150	2.6824	2.6429	1.01
250	4.5789	4.9414	0.93
350	6.5885	8.0688	0.82

Table 4. Formal potential of PPDP-PVSA determined from cyclic voltammetry.

	A-A' redox couple	
	Oxidation	Reduction
Potential (mV)	-50.7	-107.4
ΔEp (mV)	56.7	
N	1	
$E^{o'}$ (mV)	-79.05	
Randles-Sevcik Slope	-0.5197	0.6819
r^2	0.9866	0.9628
D_e ($cm^2.s^{-1}$)	9.28E-03	1.60E-02

The ipa/ipc ratio (table 3) of the system varied from 1.16 at 75 mV/s to 0.82 at 350 mV/s. Characterization of the PPDP material in 0.1 M HCl displayed peak separation (ΔEp) of 56.7 mV for the couple A-A', which indicated fully reversible electrochemistry. The diffusion coefficients of the redox couple A-A' showed that the reduction reaction was favoured for the A-A' couple (table 4)

The diffusion coefficients (D_e) of the two systems (PPDP-NQSA and PPDP-PVSA) were compared to polypyrrole systems. Literature revealed that polypyrrole diffusion coefficients were affected by temperature. Temperature ranges between 4 °C to 32 °C showed D_e between 3.29 x 10^{-10} $cm^2.s^{-1}$ to 4.04 x 10^{-10} $cm^2.s^{-1}$ [28]. Diffusion coefficient values for free standing polypyrrole systems in 0.1 M and 0.5 M $LiClO_4$ solutions displayed similar D_e values with D_e = 1.2 x 10^{-9} $cm^2.s^{-1}$ and D_e = 2.3 x 10^{-10} $cm^2.s^{-1}$ respectively [29]. Diffusion rates for the two systems evaluated in this work were much faster, with PPDP-NQSA displaying D_e = 4.62 x 10^{-7} $cm^2.s^{-1}$ (oxidation), D_e = 4.62 x 10^{-7} $cm^2.s^{-1}$ (reduction). The PPDP-PVSA system displayed greater D_e values than the PPDP-NQSA system with the D_e = 9.28 x 10^{-3} $cm^2.s^{-1}$ (oxidation) and D_e = 1.60 x 10^{-2} $cm^2.s^{-1}$ (reduction).

3.4. Electrochemical Impedance Spectroscopy

EIS data was collected in consecutive 100 mV steps, between a potential range of 100 mV to 500 mV. This potential range corresponds to the redox active window of PPDP-NQSA and was done to assess the formal potential and substantiate the value determined from square wave analysis.

The potential with the lowest impedance is the formal potential and was found to be +320 mV for this system (figure 10). This coincides with the value from square wave, i.e. +318 mV.

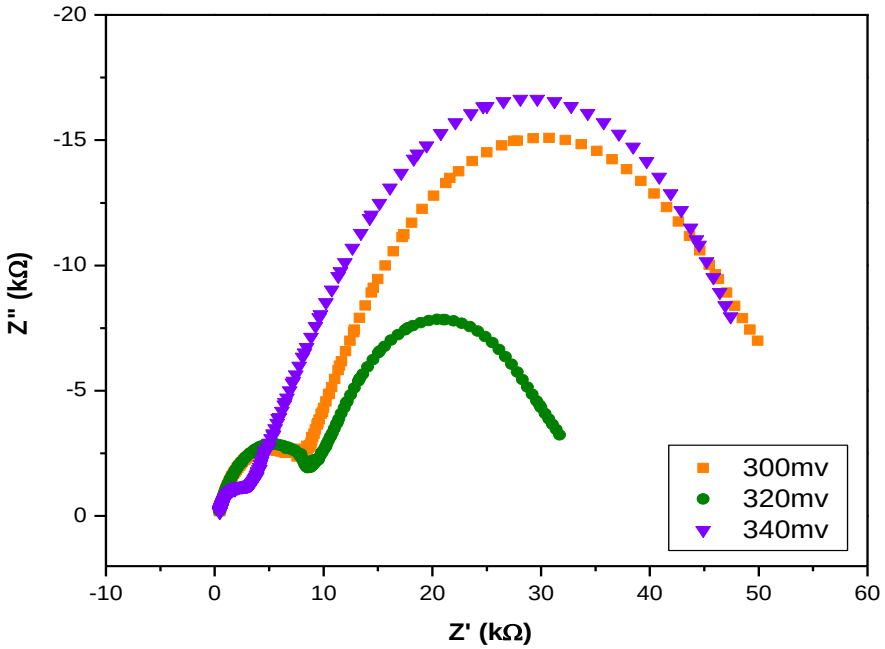

Figure 10. EIS spectra of PPDP-NQSA in 0.1M HCl from 200 mV to 350 mV vs Ag/AgCl, with 50 mV steps.

To quantitatively analyze the behaviour of PPDP films, the experimental results were fitted to an equivalent circuit, where the values of the electrical components are associated with the physical/ chemical properties of the electrochemical systems [30], using a non-linear least squares fitting method by Zahner (Thales-SIM) fitting program. The equivalent circuit (figure 11) consisted of the solution resistance (R_s) in series with $R_{ct1}C_1$ parallel combination, which is in series with $R_{ct2}CPE_2$ parallel combination. The combination $R_{ct1}C$ models the movement of electron hopping along the polymer backbone. The second component $R_{ct2}CPE_2$ represents the electrode/solution interface [31-32]. R_s is the high-frequency solution resistance, C is the double layer capacitance, R_{ct1} is the high-frequency ionic charge transfer resistance at the polymer/electrolyte interface or electron transfer resistance at the GC/electrode interface. R_{ct2} is the low-frequency electron transfer resistance of the redox reactions and CPE_2 is the constant phase element for bulk faradaic pseudo-capacitance [33].

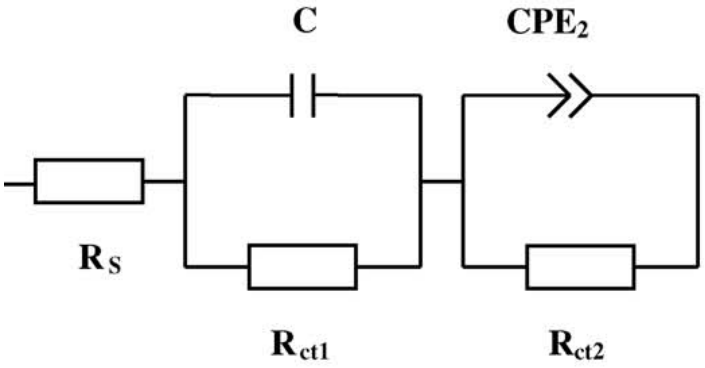

Figure 11. Equivalent circuit used to fit the results from Impedance.

The capacitance is replaced by a CPE, since polymer films have rough or porous surfaces and thus the CPE compensates for the inhomogeneity of geometry and energy at the electrode interface. Capacitance for the impedance data can be obtained from:

$$CPE = (1/ Z_{CPE}\, j\omega)^{-\alpha} \quad \ldots\ldots\ldots\ldots \text{(equation 2)}$$

where α is a fractional exponent, having values between 0 and 1, $j = \sqrt{1}$, $\omega = 2\Pi f$ is the angular frequency and Z_{CPE} is the real impedance. When α = 0 the CPE describes an ideal resistor, for α = 1 it describes an ideal capacitor and for α = 0.5 it represents homogenous semi-infinite diffusion [34-35]. The CPE also describes the distribution of relaxation times of the process occurring in the inhomogeneous polymer film [36-38]. When a CPE is parallel to a resistor, a depressed semi- circle (Cole-element) is produced [33]. The quality of the fit obtained by using different equivalent circuits was estimated by the relative errors (%) and significance of each parameter values.

The complex plane plot (Figure 12) showed two distinctive well-defined semi-circles, the smaller one in the high frequency range and the bigger one in the low frequency range. The impedance behaviour at formal potential was numerically evaluated.

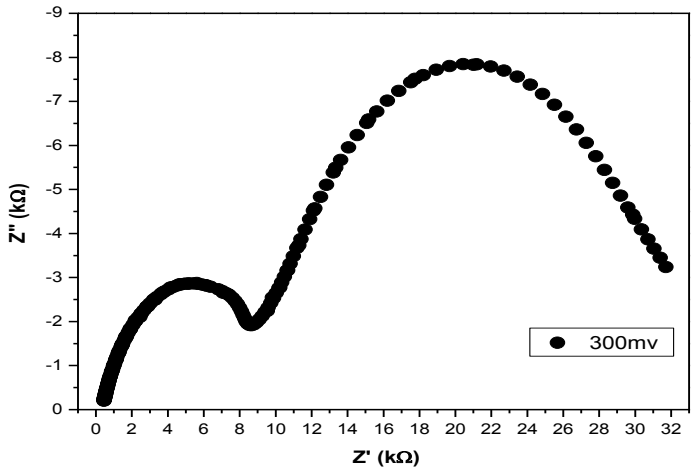

Figure 12. EIS spectra of PPDP-NQSA at 320 mV vs Ag/AgCl

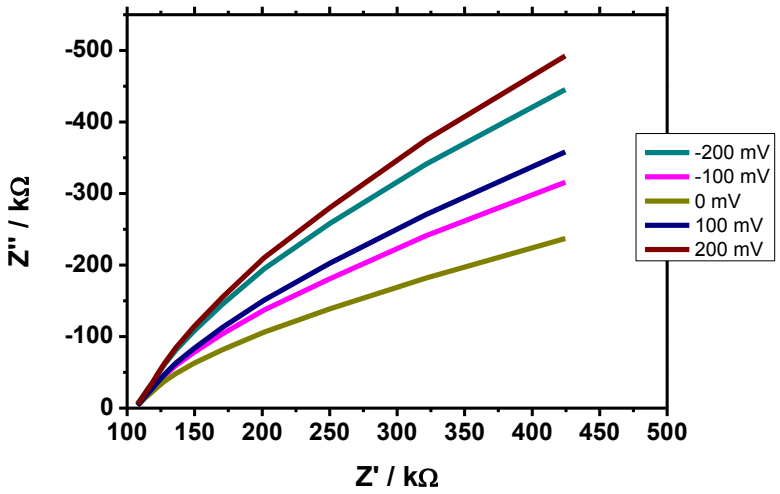

Figure 13. EIS of PPDP-PVSA in 0.1 M HCl from -200 mV to 200 mV vs Ag/AgCl, with 100 mV steps.

The Nyquist plot (figure 13) displayed a linear spectrum that never approached the Z_{RE} (real impedance) axis, but instead the systems increasingly approached large Z_{IM} (imaginary impedance) values [39]. The equivalent circuit below was used to fit the data obtained from the Impedance. The equivalent circuit consisted of a solution resistance (R_s) in series with R_pC_{PE} parallel combination, with the R_p – charge transfer resistance and C_{PE} –constant phase element (figure 14).

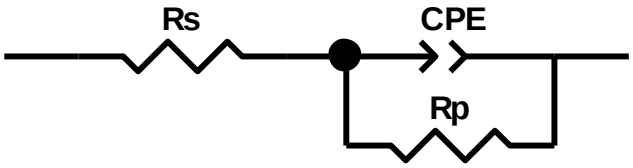

Figure 14. Equivalent circuit used to fit data from Impedance.

The components of the equivalent circuit were determined from the complex plane plot at -100 mV. The electrical equivalent circuit fitting data for the low frequency region, each system was compared for potential driven actuation response.

Table 5. Data obtained from oxidation peaks during EIS measurements

	PPPD/NQSA	PPDP/PVSA	PPDP/PVSA	PPDP/PVSA	PPDP/PVSA
potential / mV	320	-100	+100	-200	+200
Rs / Ω	333.4	105.8	106.7	106	107.4
CPE / μF	4.811	4.03	6.29	2.34	3.37
Rct / kΩ	Rct(2) = 21.6	4.056	4.094	3.547	4.094

The average charge transfer resistance (table 5) of the system was found to be 4589.45 Ω which in terms of conductivity is fairly low. Beneficial behaviour of actuation systems favour materials with high electrical conductivity to the supply the electrical input these actuation systems require for deformation. Compared to the conductivity of polypyrrole (10^{-3} to 10 $S.cm^{-1}$) these systems displayed relatively low values.

The PPDP-NQSA system displayed a lower conductivity; based on the charge transfer resistance compared to that of the PPDP-PVSA system. High conductivity is a prerequisite for a good actuator. Further investigation of the capacity behavior in the oxidized and reduced states was done on the more conductive system. The interfacial capacitance modeled as constant phase elements measured ~50 % higher capacitance values in the oxidized state compared to the reduced state for the PPDP-PVSA actuator system. This bodes well for electrochemical actuation applications at low potential.

4. CONCLUSION

FTIR and ^{1}H NMR spectroscopy revealed that the desired hinged monomer was successfully synthesized by reflux condensation. The linkage occurred at the position where the aldehyde group was attached to the pyrrole ring. ^{1}H NMR also confirmed that the linkage occurred at the position where the aldehydic carbonyl was lost. Diffusion coefficient values were evaluated from scan rate dependent cyclic voltammetry confirmed that PVSA (~10^{-3} $cm^{2}.s^{-1}$) was a better dopant than NQSA (~10^{-7} $cm^{2}.s^{-1}$) for improving electron mobility in the polymer thin films. Surface concentration values

of the both materials differed with PPDP-PVSA (~10^{-10} mol.cm^{-2} – oxidation and ~10^{-10} mol.cm^{-2} – reduction) and PPDP-NQSA (~10^{-9} mol.cm^{-2} – oxidation and ~10^{-9} mol.cm^{-2} – reduction). Electrochemical impedance spectroscopy enabled the redox dependent volume change along the polymer backbone as measured by an increase in capacitance at low frequency as the polymer changes from the reduced to the oxidized state. The PPDP-PVSA hinged polymer holds promise for electrochemical sensing based on actuation at low potential.

References

1. X.G. Li, M.R. Huang, L.X. Wang, M.F. Zhu, A. Menner, J. Springer. *Synthetic Met.* 123(2001) 435-441.
2. P.A. Mabrouk. *Synthetic Met.* 150(2005) 101-105.
3. S.M. Sayyah, E.S.S. Abd M.M. El-Deeb. *J App Polm Sci.* 90(2003) 1783-1792.
4. A. Baba, R.C. Advincula, W. Knoll. PMSE Preprints 86(2002) 48-49.
5. G. Li, Y. Wang, H, Xu. *Sensors* 7(2007) 239-250.
6. P. Burgmayer, R.W. Murray. *J Electroanal Chem Interfacial Electrochem.* 135(1982) 335-42.
7. T.F. Otero, H.J. Grande, J. Rodriguez. *J Phys Chem B.* 101(1997) 3688-3697.
8. D.Y. Lee, Y. Kim, S.J. Lee, M.H. Lee, J.Y. Lee, B.Y. Kim, N.I. Cho. *Mat Sci Eng C-Bio S.* 28(2008) 294-298.
9. T.F. Otero, J.M. Sansinena. *Adv Mater.* 10(1998) 491-494.
10. R.H. Baughman. *Synthetic Met.* 78(1996) 339-353.
11. Y. Bar-Cohen, *SPIE PRESS.* 2004.
12. A. Della Santa, D. De Rossi, A. Mazzoldi. *Synthetic Met.* 90(1997) 93-100.
13. S. Hara, T. Zama, W. Takashima, K. Kaneto. *Polym J.* 36(2004) 933-936.
14. J.D. Madden, P.G. Madden, P.A. Anquetil, I.W. Hunter. *Mater Res Soc Symp Proc* 698(2002) 137-144.
15. V. Somerset, M. Klink, R. Akinyeye, I. Michira, M. Sekota, A. Al-Ahmed, P.G.L. Baker, E. Iwuoha. *Macromol Symp.* 255(2007) 36-49
16. E. Smela. *J Micromech Microeng.* 9(1999) 1–18.
17. R.O. Akinyeye, I. Michira, M. Sekota, A. Al Ahmed, D. Tito, P.G.L. Baker, C.M.A. Brett, M. Kalaji, E. Iwuoha. *Electroanal.* 19(2007) 303-309.
18. K.A. Thomas, W.B. Euler. *J Electroanal Chem.* 501(2001) 235-240
19. S.Y. Niu, S.S. Zhang, L.B. Ma, K. Jiao. *B Kor Chem Soc.* 25(2004) 829-832.
20. R.W. Murray. *Annu Rev Mater Sci.* 14(1984) 145-69,
21. D.M. Kelly, J.G. Vos. *Electrochim Acta.* 41(1996) 1825-1832.
22. A.P. Brown, F.C. Anson. *Anal Chem.* 49(1977) 1589-95.
23. A.J. Bard, L.R. Faulkner. *Dianhuaxue.* 7(2001) 255
24. R.S. Nicholson. *Anal Chem.* 37(1965) 667-71.
25. R. Akinyeye, I. Michira, M. Sekota, A. Al-Ahmed, P.G.L. Baker, E. Iwuoha. *Electroanal.* 18(2006) 2441-2450.
26. R. Pauliukaite, C.M.A. Brett, A.P. Monkman. *Electrochim Acta.* 50(2004) 159-167.
27. F. Sundfords, J. Bobacka, A. Ivaska, A. Lewenstam, *Electrochimica Acta.* 47(2002), 2245.
28. T.F. Otero and J.G. Martinez. *J Solid State Electr.* 15(2010) 1169-1178.
29. M.J. Aniza and T.F. Otero. *Colloid Surface A.* 270-271(2005) 226-231.
30. O.E. Barcia, E. D'Elia, I. Frateur, O.R. Mattos, N. Pebere, B. Tribollet. *Electrochim Acta.* 47(2002) 2109-2116.
31. M. Grzeszczuk, G. Zabinska-Olszak. *J Electroanal Chem.* 427(1997) 169-177.

32. P.J. Mahon, G.L. Paul, S.M. Keshishian, A.M. Vassallo. *J Power Sources.* 91(2000) 68-76.
33. A. Hallik, A. Alumaa, J. Tamm, V. Sammelselg, M. Vaeaertnou, A. Jaenes, E. Lust. *Synthetic Met.* 156(2006) 488-494
34. A. Lasia. *Mod Aspec Electroc.* 32(1999) 143-248.
35. R.J. MacDonald. *J Electroanal Chem Interfacial Electrochem.* 223(1987) 25-50.
36. M. Martini, T. Matencio, N. Alonso-Vante, M. De Paoli. *J Brazil Chem Soc.* 11(2000) 50-58.
37. J. Bisquert, G. Garcia-Belmonte, F. Fabregat-Santiago, N.S. Ferriols, P. Bogdanoff, E.C. Pereira. *J Phys Chem B.* 104(2000) 2287-2298.
38. S. Krause. *Wiley-VCH*. 3(2003) 196-229.
39. A.L. Eckermann, Daniel J. Feld, Justine A. Shaw, and Thomas J. Meade. *Coordin Chem Rev.* 254(2010) 1769–1802.